ACS Medicinal Chemistry Letters

pubs.acs.org/acsmedchemlett Letter

Development of Fluorescence Imaging Probes for Labeling COX-1 in Live Ovarian Cancer Cells

Jatinder Kaur, Atul Bhardwaj, and Frank Wuest*

Cite This: ACS Med. Chem. Lett. 2021, 12, 798−804 Read Online

ACCESS | Metrics & More | Article Recommendations | Supporting Information

ABSTRACT: Recent experimental evidence demonstrated an aberrant overexpression of cyclooxygenase-1 (COX-1) in various cancers, which has stimulated the development of COX-1-selective inhibitors as promising anticancer drugs and cancer imaging agents. Herein we describe the synthesis and validation of 3-(furan-2-yl)-*N*-aryl 5-amino-pyrazoles as a novel class of COX-1 inhibitors, including molecular docking studies. Among all tested compounds, 4-(5-azido-3-(furan-2-yl)-1*H*-pyrazol-1-yl)benzoic **17** displayed a favorable COX-1 inhibition and selectivity profile (COX-1 IC_{50} = 0.1 μM, SI >1000 over COX-2). Compound **17** was selected as a lead structure for developing the novel COX-1-selective fluorescent probe **22**. Fluorescent probe **22** was prepared via click chemistry by installing a nitro-benzoxadiazole motif as a fluorophore into the 3-(furan-2-yl)-*N*-aryl 5-amino-pyrazole scaffold. Fluorescence probe **22** was tested in ovarian cancer cell line OVCAR-3, confirming its usefulness for targeting and visualizing COX-1 in living cells with confocal microscopy.

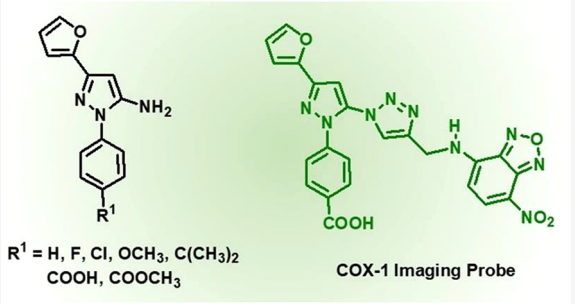

KEYWORDS: *Cyclooxygenase-1, COX-1-selective inhibitors, fluorescence imaging probe*

Cancer can evolve from various chronic inflammatory conditions associated with infections, immune-mediated diseases, and exposure to chemical and physical irritants.[1] The functional relationship between chronic inflammation and cancer development was first postulated by the German pathologist Rudolf C. Virchow in 1863.

Arachidonic-acid (AA)-derived lipid signaling molecules like prostaglandins and thromboxanes play a crucial role in the body's response to inflammatory conditions. Prostaglandins and thromboxanes are produced from polyunsaturated fatty acid AA by a set of enzymatic reactions involving cyclo-oxygenases (COXs) and specific synthases. COXs are evolutionarily conserved oxidoreductases that exist as two distinct isoforms, COX-1 and COX-2.[2−4] The role of the inducible isoform COX-2 in cancer-related inflammation has extensively been investigated in various cancer types. Typical examples include esophageal, gastrointestinal, pancreatic, breast, prostate, bladder, and colorectal cancer.[5] Unlike COX-2, the constitutively expressed isoform COX-1 has received much less consideration as a cancer biomarker and cancer drug target despite its increased expression levels in several human cancers.[6,7] In many human cancers, both isoforms exert a coordinated pathogenetic role, whereas only COX-1 plays a prominent role in some selected cases.[7] Most notably, elevated expression levels of COX-1 rather than COX-2 are detected in ovarian cancer. Ovarian cancer is the most lethal gynecologic malignancy, primarily occurring in menopausal women. Ovarian cancer ranks fifth in cancer deaths among women, and it was estimated that there were nearly 300 000 new cases in 2018. Recent studies on ovarian cancer show that COX-1, but not COX-2, plays a crucial role in tumor growth and progression by controlling prostaglandin synthesis and promoting the production of angiogenic growth factors.[8,9] COX-1 displays moderate to high expression levels in most high-grade ovarian cancers, and increased COX-1 expression is associated with a poor prognosis. The administration of the COX-1-selective inhibitor SC560 suppressed tumor growth in epithelial ovarian cancer, whereas the COX-2-selective inhibitor celecoxib showed no effect.[10] The existing experimental evidence and other findings on the elevated expression of COX-1 in skin and colon cancer make COX-1 a promising biomarker for the targeted imaging and therapy of cancer.

Early and accurate diagnosis of ovarian cancer is crucial to increase the otherwise low patient 5-year survival rate. Our research team has recently introduced immuno-PET (positron emission tomography) for targeting CA125 in ovarian cancer as a diagnostic tool to delineate the extent of the disease and to add value for treatment planning and monitoring the treatment response.[11−13] ^{64}Cu- and ^{89}Zr-labeled mAb-B43.13 also hold promise in detecting metastases and recurrent disease.[11−13]

Received: January 27, 2021
Accepted: April 7, 2021
Published: April 8, 2021

https://doi.org/10.1021/acsmedchemlett.1c00065
ACS Med. Chem. Lett. 2021, 12, 798−804

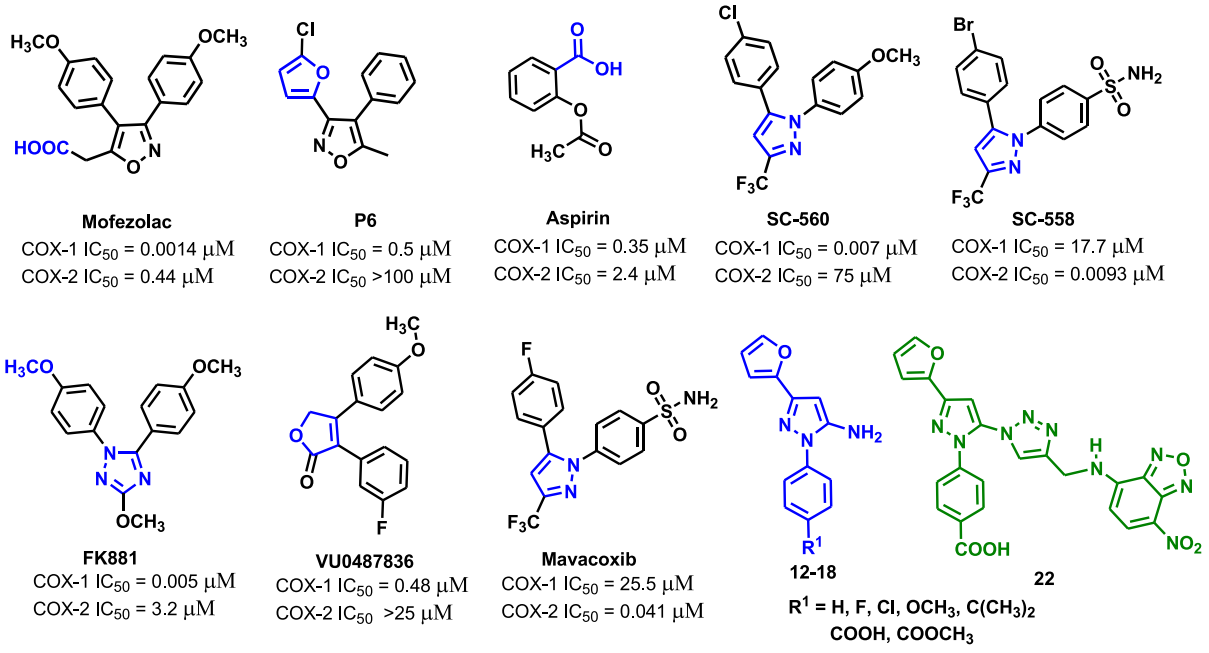

Figure 1. Selective COX-1 inhibitors containing a central five-membered heterocycle.

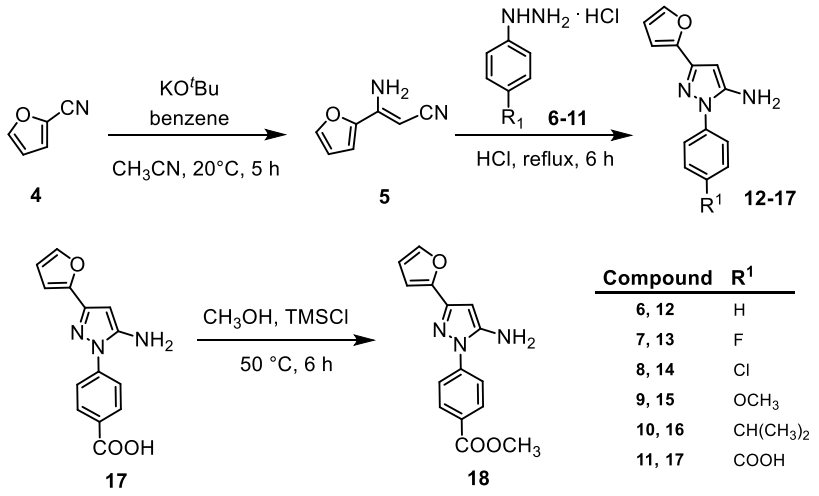

Figure 2. Synthesis of compounds **12**−**18**.

Complementary to radioimmunoconjugates for PET imaging of CA125 and [^{18}F]FDG-PET for measuring energy metabolism in ovarian cancer, the validation of other biomarkers for the noninvasive imaging of ovarian cancer is actively pursued, including COX-1. In this line, a recent study explored the potential of repurposing the ^{11}C-labeled COX-1 inhibitor [^{11}C]PS13 in rodent models of ovarian cancer for PET imaging.[14]

In addition to nuclear medicine imaging biomarkers, fluorescence imaging techniques have become a standard experimental tool in biomedical research to detect disease biomarkers and to study disease mechanisms in cells and living organisms. Fluorescence imaging with fluorescent COX-1 inhibitors represents a high-sensitivity and low-cost technique for the real-time visualization and dynamic monitoring of COX-1 as an emerging biomarker in ovarian cancer and other neoplastic diseases. Prominent examples include recently reported mofezolac-based fluorescent probes and the rhodamine-containing compound CMP for the optical imaging of COX-1 in ovarian cancer cells.[15,16]

Diarylheterocycles are among the most prominent and best-studied classes of COX-1-selective inhibitors. The structural analysis of diarylheterocycles revealed the presence of five-membered heterocycle core rings as a crucial structural motif for the design of highly potent and selective COX-1 inhibitors. Prominent examples mainly include oxazoles (mofezolac and P6) and, to a lesser extent, 1,2,4-triazoles (FK881), thiazoles (FR122047), furanones (VU487836), and pyrazoles (SC560) (Figure 1).[7,17−22]

Also, structure−activity relationship (SAR) studies and molecular docking studies demonstrated that two adjacent lipophilic aryl rings with electron-donating groups attached to an isoxazole heterocycle are critical for high affinity and COX-1-selective binding. The adjacent lipophilic aryl rings undergo several hydrophobic interactions and force the COX-1 inhibitor into a distinct position within the COX-1 binding site.[23,24]

https://doi.org/10.1021/acsmedchemlett.1c00065
ACS Med. Chem. Lett. 2021, 12, 798−804

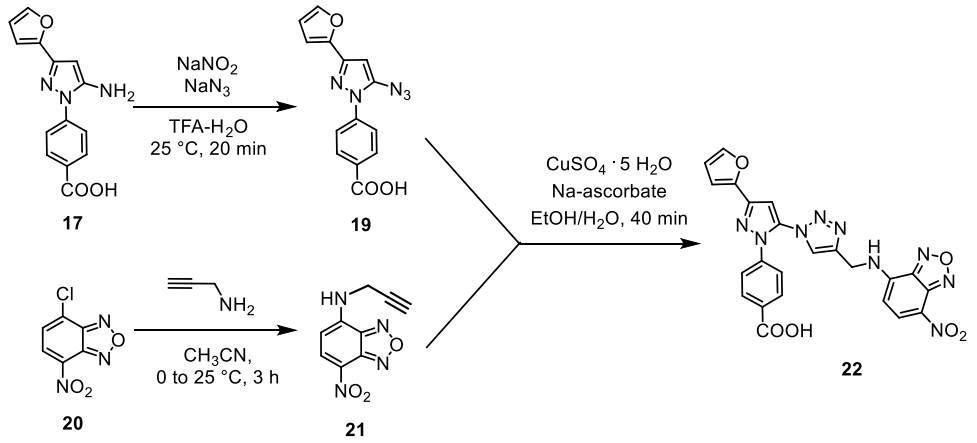

Figure 3. Synthesis of fluorescent compound **22**.

Table 1. COX-1 and COX-2 Enzyme Inhibition Data of *N*-Aryl 5-Amino-pyrazoles 12−18[a]

compd	R^1	COX-1 IC_{50} (μM)	COX-2 IC_{50} (μM)	COX-1 SI	OVCAR-3 IC_{50} (μM)	ClogP	TPSA (Å^2)
12	**H**	8.5	>100	>11	5.8	2.89	50.85
13	**F**	1.6	>100	>61	5.0	3.12	56.99
14	**Cl**	3.4	>100	>30	20.5	3.69	50.85
15	**OCH_3**	1.2	30.6	26	5.4	2.88	60.08
16	**$CH(CH_3)_2$**	2.6	>100	>38	1.1	3.37	50.85
17	**COOH**	0.10	>100	>1000	0.07	2.74	88.15
18	**$COOCH_3$**	0.19	>100	526	0.09	3.02	83.29
SC560		0.01	55.6	5560	0.008	6.18	24.83
celecoxib		>100	0.09	>1111	80.9	4.37	75.76

[a]Assays were conducted as described in the COX Inhibition Assay section of the Supporting Information. IC_{50}, half-maximal inhibitory concentration; SI, *in vitro* COX-1 selectivity index: [(COX-1 IC_{50})/(COX-2 IC_{50})]; data are the mean of three determinations. The ClogP and TPSA value were calculated using ChemDraw 16.0.

Except for compound SC560, pyrazoles generally lead to decreased COX-1 inhibitory activity and selectivity.[25] Considering the high degree of homology and structural similarity between COX-1 and COX-2 apart from the extra and crucial space in the active site of COX-2 due to the exchange of isoleucine (in COX-1) with valine (in COX-2), the failure of pyrazoles as COX-1 inhibitors contrasts the successful design of several diarylpyrazoles as highly potent and selective COX-2 inhibitors, like celecoxib, SC558, and mavacoxib.

After revisiting recent SAR and molecular docking studies with diarylheterocycles as COX-1 inhibitors, we hypothesized that the attachment of a nonadjacent furan ring at position C3 to *N*-aryl 5-amino-pyrazoles would result in a new class of potent and selective COX-1 inhibitor. To test our hypothesis, we set up the synthesis and evaluation of a series of 3-(furan-2-yl)-*N*-aryl 5-amino-pyrazoles. Moreover, the free amino group represents a suitable site for introducing additional structural motifs required to synthesize COX-1 imaging agents, including COX-1 fluorescent probes. All compounds were screened for their COX-1 and COX-2 inhibitory potency and selectivity profiles. The specific binding of fluorescent imaging probe **22** to COX-1 was tested in live ovarian cancer cells OVCAR-3 using confocal microscopy. Molecular docking studies were used to study the binding mode of compound **22** within the COX-1 binding site. The synthesis of novel COX-1 inhibitors **12−18** and fluorescence imaging probe **22** is depicted in Figures 2 and 3.

The most common method for the synthesis of substituted *N*-aryl 5-amino-pyrazoles involves the reaction of β-ketonitriles with aryl hydrazines. We envisioned the use of β-amino-acrylonitriles as masked β-ketonitrile analogs. The synthesis of *N*-aryl 5-amino-pyrazoles **12−18** commenced by the reaction of 2-furonitrile **4** with acetonitrile in the presence of KO^{t}Bu, which resulted in the formation of 3-amino-3-(furan-2-yl)acrylonitrile **5** in 81% yield. The subsequent condensation reaction of acrylonitrile **5** with arylhydrazines **6−11** gave the respective *N*-aryl 5-amino-pyrazoles **12-17** in 69−84% isolated yield.

The proposed synthesis route provides convenient access to *N*-aryl 5-amino-pyrazoles containing a furan ring at position C3 of the pyrazole ring. Carboxylic acid **17** was further converted into the corresponding methyl ester **18** in 92% yield through treatment with MeOH in the presence of TMSCl.

All of the *N*-aryl 5-amino-pyrazoles **12−18** were screened in an *in vitro* COX binding assay to assess combined different steric and electronic effects upon their COX-1 and COX-2 inhibitory potency and selectivity. Celecoxib and SC560 were used as reference compounds for high COX-2 and COX-1 inhibitory potency and selectivity. Also, *in cellulo* COX-1 inhibitory activities were determined in the COX-1-over-expressing ovarian cancer cell line OVCAR-3. The COX-1 and COX-2 inhibition data of compounds **12−18**, along with calculated *in vitro* COX-1 selectivity index (COX-1 SI), calculated lipophilicity values (CLogP), and topological polar surface area (TPSA), are summarized in Table 1.

All novel *N*-aryl 5-amino-pyrazole compounds **12−18** displayed higher inhibitory activities toward COX-1 than toward COX-2. The measured COX-1 inhibitory potencies and selectivity profiles of compounds **12−18** verify our hypothesis that *N*-aryl 5-amino-pyrazoles containing a furan

https://doi.org/10.1021/acsmedchemlett.1c00065
ACS Med. Chem. Lett. 2021, 12, 798−804

Table 2. COX-1 and COX-2 Enzyme Inhibition Data of *N*-Aryl 5-Amino-pyrazoles **19** and **22**[a]

compd	R^1	COX-1 IC_{50} (μM)	COX-2 IC_{50} (μM)	COX-1 SI	OVCAR-3 IC_{50} (μM)	Clog*P*	TPSA (Å^2)
19		0.25	>100	>400	0.4	4.32	110.89
22		0.83	>100	>120	0.9	4.79	187.88
SC560		0.01	55.6	5560	0.008	6.18	24.83
celecoxib		>100	0.09	>1111	80.9	4.37	75.76

[a]Assays were conducted as described in the COX Inhibition Assay section of the Supporting Information. IC_{50}, half-maximal inhibitory concentration; SI, *in vitro* COX-1 selectivity index: [(COX-1 IC_{50})/(COX-2 IC_{50})]; data are the mean of three determinations. The Clog*P* and TPSA value were calculated using ChemDraw 16.0.

ring at position C3 of the pyrazole ring represent a new class of COX-1-selective inhibitors. Our data also support previous reports on utilizing furan rings as alternative structural motifs to aryl rings to design potent and selective COX-1 inhibitors, as exemplified with various furan-containing isoxazoles. The replacement of the *para*-hydrogen atom in **12** with halogen atoms (fluorine in **13** and chlorine in **14**) or electron-donating groups (OMe in **15** and isopropyl in **16**) led to compounds with slightly higher COX-1 inhibitory potencies in the low micromolar range (IC_{50} = 1.2−3.4 μM) compared with parent compound **12** (IC_{50} = 8.5 μM). COX-1 selectivity profiles were moderate, as demonstrated by the COX-1 selectivity indices (SIs) of 11−61. The introduction of a carboxylic acid or ester group resulted in COX-1 inhibitors with submicromolar inhibitory potencies of 0.1 (compound **17**) and 0.19 μM (compound **18**) and higher COX-1 selectivity profiles (COX-1 SI > 1000 and 526). In addition to the obtained *in vitro* assay results, data were also verified by *in cellulo* COX-1 inhibitory experiments in COX-1-expressing ovarian cancer cells OVCAR-3.

The high inhibitory potency and COX-1 selectivity of carboxylic acid **17** agree with the structure of many traditional nonsteroidal anti-inflammatory drugs containing a carboxylic acid motif.

Typical examples include indomethacin, sulindac, and corresponding *des*-methyl derivatives, which interact with COX-1 by forming a salt bridge with R120 located at the catalytic site gate.[23]

All novel COX-1 inhibitors **12**−**18** have calculated log*P* values between 2.74 and 3.69, which fall into a more favorable lipophilicity window for drugs and imaging probes than reference compounds celecoxib and SC560. Estimated polar surface areas of *N*-aryl 5-amino-pyrazoles **12**−**18** are <90 Å^2, suggesting good cell membrane permeability capacity to reach the integral membrane protein COX-1 located in the inner membrane of the endoplasmic reticulum.

COX-1 inhibitory potency and selectivity data point to carboxylic acid **17** as the lead compound for designing a COX-1-selective fluorescent probe. Our group has demonstrated the power of click chemistry to generate highly potent and selective COX-2 inhibitors, including *in situ* click chemistry with COX-2 enzyme as a chemical template.[26] An amine group at position C5 of the pyrazole ring provides an excellent site for introducing a fluorescent tag via click chemistry using Cu(I)-catalyzed azide−alkyne cycloaddition (CuAAC). For this purpose, we converted amine **18** into corresponding azide **19** as a suitable click-chemistry building block entailing the COX-1 binding scaffold. The installation of an azide group was accomplished through a diazotization reaction with amine **18** followed by treatment with sodium azide. Azide compound **19** was prepared in 75% yield.

In previous studies, our research group has successfully used the nitro-benzoxadiazole (NBD) motif as an appropriate fluorophore for biological studies of hexose transporters and COX-2 in various breast and colorectal cancer cell lines due to its small size, strong fluorescence, and high chemical versatility.[27−30] NBD motifs undergo facile nucleophilic aromatic substitution reactions starting from commercially available nonfluorescent fluoro- or chloro-substituted NBD starting materials. We prepared complementary click chemistry building block 7-nitro-*N*-(prop-2-yn-1-yl)benzo-[*c*][1,2,5]-oxadiazol-4-amine (NBD-alkyne, **21**) in 76% yield through the reaction of 4-chloro-7-nitrobenzoxadiazole **20** with propargylamine. The application of CuAAC reaction conditions between azide **19** and alkyne **20** afforded fluorescent compound 4-(3-(furan-2-yl)-5-(4-(((7-nitrobenzo-[*c*][1,2,5]-oxadiazol-4-yl)amino)methyl)-1*H*-1,2,3-triazol-1-yl)-1*H*-pyrazol-1-yl)benzoic acid **22** in 81.5% yield. The synthesis of azide **19**, alkyne **20**, and fluorescent compound **22** is depicted in Figure 3.

Compounds **19** and **22** were also screened for their COX-1 inhibitory potency and selectivity profiles. The results are summarized in Table 2.

The conversion of the amino group in compound **17** into an azide group had no drastic effect on inhibitory potency or COX-1 selectivity. Azide-containing compound **19** still exhibited submicromolar inhibitory potency and high selectivity toward COX-1 (IC_{50} = 0.25 μM, SI >400). However, we noticed a slight decrease in the COX-1 inhibitory potency for fluorescent compound **22** (IC_{50} = 0.83 μM, SI >120), which can be attributed to the increase in the molecular size.

The introduction of the NBD fluorescence tag also increased the lipophilicity and polar surface area of compound **22** compared with *N*-aryl 5-amino-pyrazole **17**. Nevertheless, the submicromolar inhibitory potency of fluorescent probe **22** still warrants its testing for targeting and visualizing COX-1 in live ovarian cancer cells. *In vitro* binding assay data for compounds **19** and **22** were confirmed by *in cellulo* experiments with OVCAR-3 and HCA-7 cells. Fluorescence imaging of COX-1 with compound **22** was performed by confocal microscopy experiments in living cancer cells. The results of confocal microscopy experiments in COX-1 expressing OVCAR-3 cells are summarized in Figure 4.

The human ovarian cancer cell line OVCAR-3 has high baseline expression levels of COX-1 while lacking COX-2 expression, making OVCAR-3 cells an ideal cell line for validating the COX-1-selective fluorescent probe **22**.[15] Compound **22** at various concentrations (1−10 μM) was incubated with live OVCAR-3 cells at 37 °C in a temperature-controlled humidified imaging chamber installed on a confocal microscope. Significant perinuclear fluorescence staining was observed with compound **22** at 10 μM in OVCAR-3 cells. No

https://doi.org/10.1021/acsmedchemlett.1c00065
ACS Med. Chem. Lett. 2021, 12, 798−804

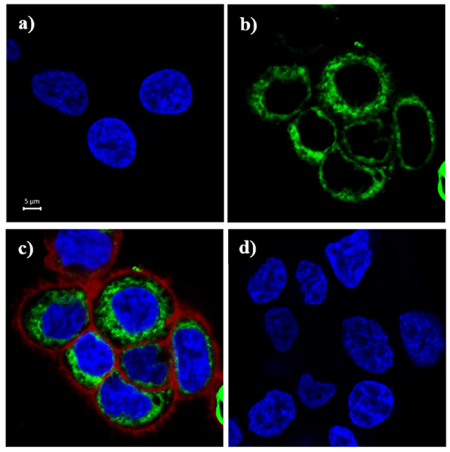

Figure 4. Confocal microscopy experiments with fluorescence imaging probe **22** in OVCAR-3 cells. Cells were treated with (a) PBS (control) and (b–d) 10 μM of **22**. (b) COX-1 staining due to the cellular uptake of **22** (nuclear staining not shown). (c) Merged image showing nuclei (blue) and COX-1 staining (green) as a result of the cellular uptake of conjugate **22** and cell membrane labeling (red). (d) OVCAR-3 cells were pretreated with 50 μM of SC560 before the treatment with **22**. All images are on the same scale as that indicated in panel a.

fluorescence signal was detected after OVCAR-3 cells were incubated with phosphate-buffered saline (PBS) as a control using similar experimental conditions. The COX-1 specificity of compound **22** was verified through specific blocking experiments. Blocking experiments involved the pretreatment of OVCAR-3 cells with the potent and specific COX-1 inhibitor SC560 at a 50 μM concentration for 20 min before the addition of fluorescence probe **22**.

The COX-1 specificity of compound **22** was also confirmed by confocal microscopy experiments in human colorectal cancer cell line HCA-7. HCA-7 expresses COX-2 but not COX-1.[31] Consequently, the treatment of COX-1-negative HCA-7 cells with 10 μM of compound **22** resulted in no detectable fluorescence signal using the same experimental conditions as those with the COX-1-positive ovarian cancer cell line OVCAR-3 (Supporting Information Figure S1). Overall, confocal microscopy experiments summarized in Figure 4 confirm the usefulness of compound **22** as a fluorescence imaging probe for targeting and detecting COX-1 in live cells.

The binding mode of compounds **17** and **22** in COX-1 active was further elucidated with molecular docking studies (Figure 5). The furan ring in compound **17** showed $\pi-\pi$ interactions with the aromatic ring of Y355, and the oxygen atom of the furan ring also showed strong hydrogen-bonding interactions with Y355 (1.4 Å). Moreover, the oxygen atom of the furan ring was found in close proximity to one of the amino groups of the R120 residue (O···NH_2 = 3.1 Å). The carboxylate group of compound **17** also indicated weak hydrogen bonding with Y385 (O···OH = 3.0 Å). All of these strong protein–ligand interactions support the experimental COX-1 inhibitory activity data of compound **17**. Molecular docking analysis results for imaging probe **22** showed that the ligand could attain a favorable binding mode in the COX-1 binding site. We also observed various hydrogen-bonding interactions with critical amino acid residues of the COX-1 binding site. One of the nitrogen atoms of the triazole ring showed hydrogen bonding with Y355 (N···OH = 3.0 Å). The oxygen atom in the NBD ring also undergoes hydrogen bonding with Y355 (O···OH = 2.01 Å) and with R120 (O···NH_2 = 2.2 Å).

In conclusion, we have synthesized and tested a series of 3-(furan-2-yl)-*N*-aryl 5-amino-pyrazoles as a novel class of COX-1-selective inhibitors. Compound **17** was identified as a promising novel COX-1 inhibitor exhibiting submicromolar COX-1 inhibitory potency and a high COX-1 selectivity profile.

Molecular docking studies further demonstrated the crucial hydrogen-bonding interactions of **17** with the amino acid residues of the COX-1 active site enabling a favorable arrangement of compound **17** in the COX-1 binding site. Compound **17** was selected as the lead structure for the development of a novel COX-1-selective fluorescent probe **22**. The COX-1-selective fluorescent probe **22** was prepared via click chemistry by installing an NBD motif as a fluorophore into the 3-(furan-2-yl)-*N*-aryl 5-amino-pyrazole scaffold. Fluorescent probe **22** was tested in ovarian cancer cell line OVCAR-3, confirming its usefulness for targeting and visualizing COX-1 in living cells with confocal microscopy.

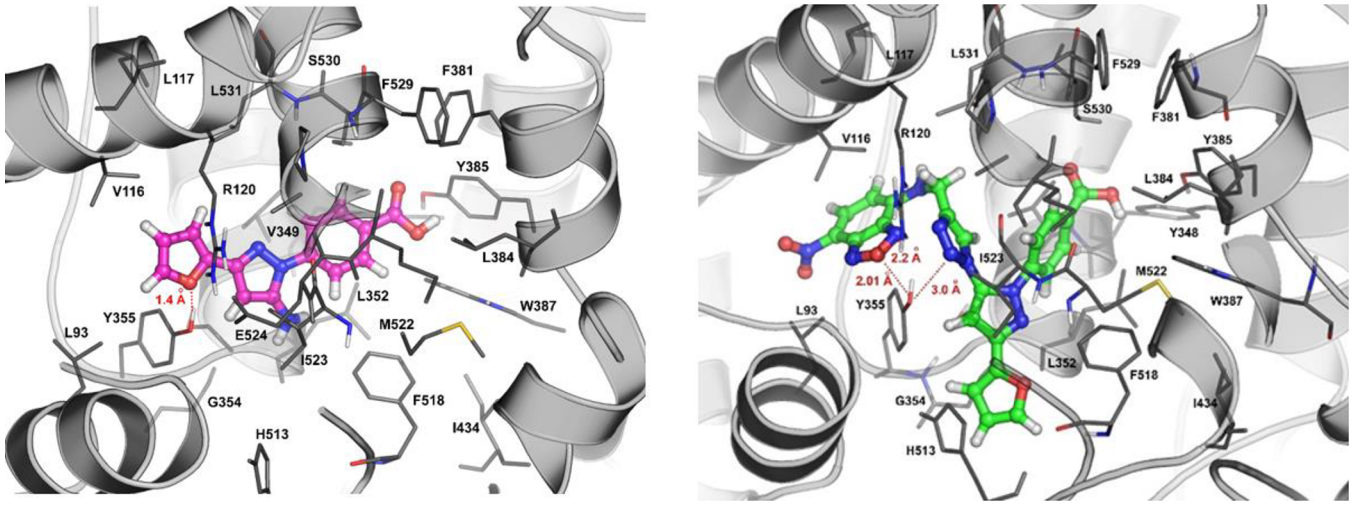

Figure 5. Molecular docking of compounds **17** (left) and **22** (right) in the COX-1 isozyme binding site (PDB ID: 1EQG).

https://doi.org/10.1021/acsmedchemlett.1c00065
ACS Med. Chem. Lett. 2021, 12, 798–804

COX-1 binding data of compounds **17**, **19**, and **22**, live-cell imaging experiments with fluorescent probe **22** and molecular docking studies with compounds **17** and **22** demonstrated the suitability of the 5-amino group as a versatile site for the preparation of additional high-affinity and selective COX-1 inhibitors and imaging probes, including radiolabeled compounds.

■ ASSOCIATED CONTENT

Supporting Information

The Supporting Information is available free of charge at https://pubs.acs.org/doi/10.1021/acsmedchemlett.1c00065.

Synthetic procedures, analytical data, assay protocols, fluorescence imaging protocols, and docking analysis procedure (PDF)

■ AUTHOR INFORMATION

Corresponding Author

Frank Wuest − *Department of Oncology, University of Alberta, Edmonton, Alberta T6G 1Z2, Canada; Faculty of Pharmacy and Pharmaceutical Sciences and Department of Chemistry, University of Alberta, Edmonton, Alberta T6G 2H7, Canada;* orcid.org/0000-0002-6705-6450; Email: wuest@ualberta.ca

Authors

Jatinder Kaur − *Department of Oncology, University of Alberta, Edmonton, Alberta T6G 1Z2, Canada; Faculty of Pharmacy and Pharmaceutical Sciences, University of Alberta, Edmonton, Alberta T6G 2H7, Canada*

Atul Bhardwaj − *Department of Oncology, University of Alberta, Edmonton, Alberta T6G 1Z2, Canada; Faculty of Pharmacy and Pharmaceutical Sciences, University of Alberta, Edmonton, Alberta T6G 2H7, Canada*

Complete contact information is available at: https://pubs.acs.org/10.1021/acsmedchemlett.1c00065

Author Contributions

J.K. conceived the idea and designed, synthesized, and characterized all compounds. J.K. designed and performed *in vitro* and cell-based biological experiments, including confocal imaging. A.B. performed computational studies. J.K. and A.B. wrote the manuscript and compiled the Supporting Information. J.K., A.B., and F.W. analyzed the data, discussed the results, and contributed to the editing of the manuscript. All authors have given approval to the final version of the manuscript.

Notes

The authors declare no competing financial interest.

■ ACKNOWLEDGMENTS

We gratefully acknowledge the Dianne and Irving Kipnes Foundation, the Canadian Institute for Health Research (CIHR), and the National Science and Engineering Research Council of Canada (NSERC) for supporting this work. F.W. and J.K. thank the Alberta Cancer Foundation (ACF) for a postdoctoral fellowship.

■ ABBREVIATIONS

COX, cyclooxygenase; COX-1, cyclooxygenase-1; COX-2, cyclooxygenase-2; NBD, nitro-benzoxadiazole; AA, arachidonic acid; PET, positron emission tomography; SAR, structure−activity relationship; SI, selectivity index

■ REFERENCES

(1) Coussens, L. M.; Werb, Z. Inflammation and cancer. *Nature* **2002**, *420* (6917), 860−867.

(2) Smith, W. L.; Urade, Y.; Jakobsson, P. J. Enzymes of the cyclooxygenase pathways of prostanoid biosynthesis. *Chem. Rev.* **2011**, *111*, 5821−5865.

(3) van der Donk, W. A.; Tsai, A. L.; Kulmacz, R. J. The cyclooxygenase reaction mechanism. *Biochemistry* **2002**, *41*, 15451−15458.

(4) Blobaum, A. L.; Marnett, L. J. Structural and functional basis of cyclooxygenase inhibition. *J. Med. Chem.* **2007**, *50*, 1425−1441.

(5) Wang, D.; DuBois, R. N. Eicosanoids and cancer. *Nat. Rev. Cancer* **2010**, *10*, 181−193.

(6) Yang, Y.; Tang, L.-Q.; Wei, W. Prostanoids receptors signaling in different diseases/cancers progression. *J. Recept. Signal Transduction Res.* **2013**, *33* (1), 14−27.

(7) Pannunzio, A.; Coluccia, M. Cyclooxygenase-1 (COX-1) and COX-1 Inhibitors in Cancer: A Review of Oncology and Medicinal Chemistry Literature. *Pharmaceuticals* **2018**, *11* (4), 101.

(8) Gupta, R. A.; Tejada, L. V.; Tong, B. J.; Das, S. K.; Morrow, J. D.; Dey, S. K.; DuBois, R. N. Cyclooxygenase-1 is overexpressed and promotes angiogenic growth factor production in ovarian cancer. *Cancer Res.* **2003**, *63*, 906−911.

(9) Perrone, M. G.; Luisi, O.; De Grassi, A.; Ferorelli, S.; Cormio, G.; Scilimati, A. Translational Theragnosis of Ovarian Cancer: where do we stand? *Curr. Med. Chem.* **2020**, *27* (34), 5675−5715.

(10) Daikoku, T.; Wang, D.; Tranguch, S.; Morrow, J. D.; Orsulic, S.; DuBois, R. N.; Dey, S. K. Cyclooxygenase-1 is a potential target for prevention and treatment of ovarian epithelial cancer. *Cancer Res.* **2005**, *65* (9), 3735−3744.

(11) Sharma, S. K.; Wuest, M.; Wang, M.; Glubrecht, D.; Andrais, B.; Lapi, S. E.; Wuest, F. Immuno-PET of epithelial ovarian cancer: harnessing the potential of CA125 for non-invasive imaging. *EJNMMI Res.* **2014**, *4* (1), 60.

(12) Sharma, S. K.; Wuest, M.; Way, J. D.; Bouvet, V. R.; Wang, M.; Wuest, F. Synthesis and pre-clinical evaluation of an (18)F-labeled single-chain antibody fragment for PET imaging of epithelial ovarian cancer. *Am. J. Nucl. Med. Mol. Imaging.* **2016**, *6* (3), 185−198.

(13) Sharma, S. K.; Sevak, K. K.; Monette, S.; Carlin, S. D.; Knight, J. C.; Wuest, F. R.; Sala, E.; Zeglis, B. M.; Lewis, J. S. Preclinical ^{89}Zr Immuno-PET of High-Grade Serous Ovarian Cancer and Lymph Node Metastasis. *J. Nucl. Med.* **2016**, *57* (5), 771−776.

(14) Boyle, A. J.; Tong, J.; Zoghbi, S.; Pike, V. W.; Innis, R.; Vasdev, N. Repurposing [11C]PS13 for PET imaging of cyclooxygenase-1 (COX-1) in ovarian cancer xenograft mouse models. *J. Nucl. Med.* **2020**, jnumed.120.249367.

(15) Scilimati, A.; Ferorelli, S.; Iaselli, M. C.; Miciaccia, M.; Pati, M. L.; Fortuna, C. G.; Aleem, A. M.; Marnett, L. J.; Perrone, M. G. Targeting COX-1 by mofezolac-based fluorescent probes for ovarian cancer detection. *Eur. J. Med. Chem.* **2019**, *179*, 16−25.

(16) Malerba, P.; Crews, B. C.; Ghebreselasie, K.; Daniel, C. K.; Jashim, E.; Aleem, A. M.; Salam, R. A.; Marnett, L. J.; Uddin, M. J. Targeted Detection of Cyclooxygenase-1 in Ovarian Cancer. *ACS Med. Chem. Lett.* **2020**, *11* (10), 1837−1842.

(17) Di Nunno, L.; Vitale, P.; Scilimati, A.; Tacconelli, S.; Patrignani, P. Novel synthesis of 3,4-diarylisoxazole analogues of valdecoxib: reversal cyclooxygenase-2 selectivity by sulfonamide group removal. *J. Med. Chem.* **2004**, *47*, 4881−4890.

(18) Vitale, P.; Perrone, M. G.; Malerba, P.; Lavecchia, A.; Scilimati, A. Selective COX-1 inhibition as a target of theranostic novel diarylisoxazoles. *Eur. J. Med. Chem.* **2014**, *74*, 606−618.

(19) Cingolani, G.; Panella, A.; Perrone, M. G.; Vitale, P.; Di Mauro, G.; Fortuna, C. G.; Armen, R. S.; Ferorelli, S.; Smith, W. L.; Scilimati, A. Structural basis for selective inhibition of Cyclooxygenase-1 (COX-1) by diarylisoxazoles mofezolac and 3-(5-chlorofuran-2-yl)-5-methyl-4-phenylisoxazole (P6). *Eur. J. Med. Chem.* **2017**, *138*, 661−668.

(20) Uddin, M. J.; Wilson, A. J.; Crews, B. C.; Malerba, P.; Uddin, M. I.; Kingsley, P. J.; Ghebreselasie, K.; Daniel, C. K.; Nickels, M. L.; Tantawy, M. N.; Jashim, E.; Manning, H. C.; Khabele, D.; Marnett, L. J. Discovery of Furanone-Based Radiopharmaceuticals for Diagnostic Targeting of COX-1 in Ovarian Cancer. *ACS Omega* **2019**, *4* (5), 9251−9261.
(21) Imanishi, J.; Morita, Y.; Yoshimi, E.; Kuroda, K.; Masunaga, T.; Yamagami, K.; Kuno, M.; Hamachi, E.; Aoki, S.; Takahashi, F.; Nakamura, K.; Miyata, S.; Ohkubo, Y.; Mutoh, S. Pharmacological profile of FK881 (ASP6537), a novel potent and selective cyclooxygenase-1 inhibitor. *Biochem. Pharmacol.* **2011**, *82*, 746−754.
(22) Vitale, P.; Tacconelli, S.; Perrone, M. G.; Malerba, P.; Simone, L.; Scilimati, A.; Lavecchia, A.; Dovizio, M.; Marcantoni, E.; Bruno, A.; Patrignani, P. Synthesis, pharmacological characterization, and docking analysis of a novel family of diarylisoxazoles as highly selective cyclooxygenase-1 (COX-1) inhibitors. *J. Med. Chem.* **2013**, *56* (11), 4277−4299.
(23) Vitale, P.; Panella, A.; Scilimati, A.; Perrone, M. G. COX-1 Inhibitors: Beyond Structure Toward Therapy. *Med. Res. Rev.* **2016**, *36* (4), 641−671.
(24) Vitale, P.; Perrone, M. G.; Malerba, P.; Lavecchia, A.; Scilimati, A. Selective COX-1 inhibition as a target of theranostic novel diarylisoxazoles. *Eur. J. Med. Chem.* **2014**, *74*, 606−618.
(25) Perrone, M. G.; Vitale, P.; Malerba, P.; Altomare, A.; Rizzi, R.; Lavecchia, A.; Di Giovanni, C.; Novellino, E.; Scilimati, A. Diarylheterocycle core ring features effect in selective COX-1 inhibition. *ChemMedChem* **2012**, *7* (4), 629−641.
(26) Bhardwaj, A.; Kaur, J.; Wuest, M.; Wuest, F. In situ click chemistry generation of cyclooxygenase-2 inhibitors. *Nat. Commun.* **2017**, *8*, 1−13.
(27) Tietz, O.; Kaur, J.; Bhardwaj, A.; Wuest, F. Pyrimidine-based fluorescent COX-2 inhibitors: synthesis and biological evaluation. *Org. Biomol. Chem.* **2016**, *14* (30), 7250−7257.
(28) Kaur, J.; Bhardwaj, A.; Wuest, F. In Cellulo Generation of Fluorescent Probes for Live-Cell Imaging of Cylooxygenase-2. *Chem. - Eur. J.* **2021**, *27* (10), 3326−3337.
(29) Bhardwaj, A.; Kaur, J.; Wuest, F.; Knaus, E. E. Fluorophore-labeled cyclooxygenase-2 inhibitors for the imaging of cyclooxygenase-2 overexpression in cancer: synthesis and biological studies. *ChemMedChem* **2014**, *9* (1), 109−240.
(30) Soueidan, O. M.; Scully, T. W.; Kaur, J.; Panigrahi, R.; Belovodskiy, A.; Do, V.; Matier, C. D.; Lemieux, M. J.; Wuest, F.; Cheeseman, C.; West, F. G. Fluorescent Hexose Conjugates Establish Stringent Stereochemical Requirement by GLUT5 for Recognition and Transport of Monosaccharides. *ACS Chem. Biol.* **2017**, *12* (4), 1087−1094.
(31) Tietz, O.; Wuest, M.; Marshall, A.; Glubrecht, D.; Hamann, I.; Wang, M.; Bergman, C.; Way, J. D.; Wuest, F. PET imaging of cyclooxygenase-2 (COX-2) in a pre-clinical colorectal cancer model. *EJNMMI Res.* **2016**, *6* (1), 37.

https://doi.org/10.1021/acsmedchemlett.1c00065
ACS Med. Chem. Lett. 2021, 12, 798−804